J|A|C|S COMMUNICATIONS

Published on Web 12/02/2009

Direct Atomic-Scale Observation of Redox-Induced Cation Dynamics in an Oxide-Supported Monolayer Catalyst: WO_x/α-$Fe_2O_3(0001)$

Zhenxing Feng,[†] Chang-Yong Kim,[§] Jeffrey W. Elam,[||] Qing Ma,[‡] Zhan Zhang,[⊥] and Michael J. Bedzyk*,[†,#]

Department of Materials Science and Engineering, Institute for Catalysis in Energy Processes, and DND-CAT, Synchrotron Research Center, Northwestern University, Evanston, Illinois 60208, Canadian Light Source Inc., Saskatoon, SK, Canada S7N 0X4, and Energy Systems Division, X-ray Science Division, and Materials Science Division, Argonne National Laboratory, Argonne, Illinois 60439

Received August 11, 2009; E-mail: bedzyk@northwestern.edu

Metal oxide monolayers or clusters anchored to an oxide support are important catalysts for industrial processes.[1] Typically, a catalyst exhibits greater activity as a monolayer (ML) than as a thicker film.[2] More importantly, predictability of the interface structure of the supported oxide would have an enormous impact upon our understanding of numerous chemical processes, since the structure of the catalyst affects chemical reactions, as, for example, in the proposed case of NO decomposition.[3] Herein, we demonstrate with atomic-scale sensitivity how to follow the redox-induced surface-site exchange of cations on an oxide support as well as the concurrent changes in the oxidation states of the supported cations. To accomplish this, we have used in situ X-ray standing-wave (XSW) three-dimensional (3D) atomic imaging[4,5] combined with ex situ X-ray photoelectron spectroscopy (XPS) and X-ray absorption fine structure (XAFS) measurements.

In this study, we monitored the reversible changes during the redox cycle of a $^1/_3$ ML WO_x/α-$Fe_2O_3(0001)$ interface grown by atomic layer deposition (ALD). W atomic maps and XPS spectra were recorded for the as-deposited (AD), oxidized (Ox), and reduced (Re) interfaces. Reversibility was demonstrated by observing that the results of the reoxidized (Ox2) interface matched those of the Ox surface. While redox-induced chemical shifts in XPS for catalytically active cations are well-known,[6] there are (to our knowledge) no predictions or measurements that clearly show redox-induced cation migration from one surface symmetry site to another. Our present study of a $^1/_3$ ML WO_x/α-$Fe_2O_3(0001)$ interface is the first report in which a surface reaction has been observed to cause a complete migration of a ML or sub-ML species from one surface site to another surface site that is symmetry-inequivalent.

For this study, a polished hematite(0001) mineral single crystal was oxygen-annealed and exposed to a single ALD growth cycle that used WF_6 [see the Supporting Information (SI) for details]. Atomically flat terraces were observed by atomic-force microscopy (AFM) before and after the ALD and after the redox treatment. The sample was removed from the ALD reactor and placed inside a beryllium-dome reaction chamber that was mounted on a diffractometer for in situ XSW measurements at the Advanced Photon Source (APS) 5ID-C station. A W coverage of 0.31 ML was determined by X-ray fluorescence (XRF). The sample was measured by XSW in the AD, Ox, Re, and Ox2 conditions. The Ox and Re surfaces were prepared by annealing at 350 °C in pure O_2 and 2% H_2 in He, respectively. Ex situ XPs spectra (Figure S2 in the SI) of the W 4f doublet peaks for the AD, Ox, and Re surfaces along with peak fits[6,7] show that the AD surface has a 30% W^{5+} [binding energy (BE) = 34.5 and 36.6 eV] and 70% W^{6+} (BE = 35.5 and 37.6 eV), while the Ox surface has 100% W^{6+} and the Re surface 90% W^{5+} and 10% W^{6+}. The Fe 2p XPS spectra (Figure S2) indicate that the chemical state of the Fe cations at the interface did not change.

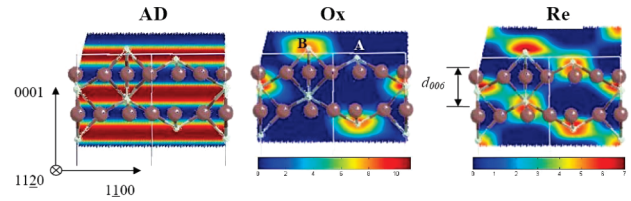

Figure 1. (11$\bar{2}$0) 2D cuts through the XSW-measured 3D W atomic density maps for the AD, Ox, and Re WO_x/α-$Fe_2O_3(0001)$ interfaces and projections of the α-Fe_2O_3 ball-and-stick model. The small white balls represent Fe cations, and the larger brown balls are O anions. The map for the Ox surface is recovered after a second oxidation.

The single-crystal XSW method uses dynamical Bragg diffraction to generate an *E*-field intensity pattern below[8] and above[9] the surface that has a periodicity equivalent to the diffraction planes. Analysis of the characteristic XRF modulation from a surface adatom species while scanning through the $\mathbf{H} = hkl$ Bragg reflection produces the Fourier amplitude ($f_\mathbf{H}$) and phase ($P_\mathbf{H}$) of that atom's distribution. The XSW method has been reviewed elsewhere.[4,10,11] The Fourier summation with these measured amplitudes and phases generates a model-independent 3D map, $\rho(\mathbf{r})$, for the XRF-selected atomic species:[5,7,12]

$$\rho(\mathbf{r}) = 1 + 2 \sum_{\mathbf{H}\neq-\mathbf{H},\mathbf{H}\neq0} f_\mathbf{H} \cos[2\pi P_\mathbf{H} - \mathbf{H}\cdot\mathbf{r}] \qquad (1)$$

The XSW W L fluorescence data and analysis for the AD, Ox, and Re surfaces show striking differences (Figure S5). The measured $f_\mathbf{H}$ and $P_\mathbf{H}$ values (Table S1) show that the W atomic distribution for the AD surface is vertically correlated but laterally uncorrelated to the substrate lattice, whereas the Ox and Re surfaces are 3D-correlated. The Ox and Re W Fourier components are similar in the (0006) normal direction but significantly different in the two off-normal directions. This indicates lateral differences in the W distribution. Furthermore, Ox2 gives almost the same $f_\mathbf{H}$ and $P_\mathbf{H}$ as Ox, indicating reversibility of this redox reaction.

By inserting the XSW-measured Fourier components into eq 1, we generated the 3D W atomic density maps shown in Figure 1. For purposes of registry, Figure 1 shows cuts of the measured W maps superimposed on the projection of the α-Fe_2O_3 substrate ball-and-stick model. For the α-$Fe_2O_3(0001)$ surface, there are two symmetry-inequivalent Fe sites, A and B, above the topmost oxygen layer. These are symmetrically equivalent to the two occupied Fe octahedral sites in the bulk. The A site is located closer to its

[†] Institute for Catalysis in Energy Processes, Northwestern University.
[‡] Synchrotron Research Center, Northwestern University.
[§] Canadian Light Source Inc.
[||] Energy Systems Division, Argonne National Laboratory.
[⊥] X-ray Science Division, Argonne National Laboratory.
[#] Materials Science Division, Argonne National Laboratory.

10.1021/ja906816y

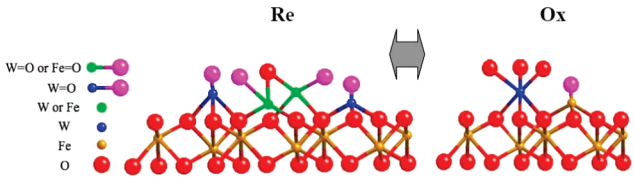

Figure 2. Proposed models for the fully reduced (Re) and oxidized (Ox) WO_x/α-$Fe_2O_3(0001)$ interfaces that are consistent with the XSW-measured W atomic maps and the 5+ and 6+ oxidation states found by XPS.

Table 1. Best-fit Parameters for the W Adsorption Geometry Model, Where c_X and z_X Are the W Occupation Fraction and Height, Respectively, for Site X (X = A, B); For Comparison, Fe in Bulklike α-Fe_2O_3 Has $z_A = 0.85$ Å and $z_B = 1.45$ Å

surface	c_A	c_B	z_A (Å)[a]	z_B (Å)[a]
Ox	0.04(1)	0.64(1)	–	1.58(2)
Re	0.31(1)	0.36(1)	0.88(3)	1.46(2)
Ox2	0.05(7)	0.61(8)	–	1.54(7)

[a] $z = 0$ is at the bulklike oxygen plane.

underlying oxygen trimer than the B site. The 3D W maps show that for the Ox surface, W^{6+} cations occupy only B sites, while in the reduced state, tungsten cations occupy both A and B sites.

Figure 2 shows our proposed models for explaining the above observations. These models are partially based on our earlier study of VO_x/α-$Fe_2O_3(0001)$.[12] For the Ox surface, our model shows W in the Fe B site, as measured by XSW, and proposes a local structure similar to the WO_3 tetragonal crystal structure, which is composed of six W−O bonds with some distortion. This local structure is based on a comparison of our XAFS measurements for the Ox sample with those for a standard WO_3 powder sample (Figures S6 and S7). The reduced state is more complex, since the XSW map shows W^{5+} cations in both the A and B sites. Figure 2 illustrates a few possible structures: isolated WO_4 in either A or B sites, with one W═O bond above the surface and three W−O-substrate bonds, or a dimer structure as proposed in ref 12, with W replacing V.

To quantify the W occupation fractions (c_X) and heights (z_X) for sites A and B in the Ox, Re, and Ox2 states, we used a least-squares global fit of a model to the set of measured Fourier components for the W atomic distribution:

$$F_H = f_H \exp(2\pi i P_H) = c_A \exp[2\pi i(2h + k + 3lz_A)/3] + c_B \exp[2\pi i(h + 2k + 3lz_B)/3]. \quad (2)$$

The parameters from the best fits, which are listed in Table 1, quantitatively show the movement of W cations during redox reactions. In this table, $c_A + c_B \approx 0.7$, indicating that 70% of the total W are ordered in both redox states. The remaining W atoms are measured to be in an uncorrelated distribution relative to the substrate lattice. Since AFM and grazing-incidence small-angle X-ray scattering (at APS 12ID-C) showed no evidence of nanocluster formation, the uncorrelated W cations are most likely associated with hematite surface defect sites and step edges. Table 1 also shows that in the Ox state, all of the ordered W cations are at B sites. However, the reduction causes half of those ordered W cations to migrate from B sites to A sites. Ox2 moves all W cations in A sites back to B sites. The W heights in the A and B sites are close to the original bulklike Fe heights of 0.85 and 1.45 Å, respectively.

We now propose explanations for the AD, Ox, and Re structures and the dynamics that occur in the transitions between these states. We start with the assumption that the bare hematite(0001) surface is Fe═O terminated with B sites unoccupied and A sites occupied by Fe in an O−Fe−O_3−Fe··· configuration, as predicted by density functional theory[13,14] and observed by scanning tunneling microscopy.[15] (This configuration can be seen in Figure 2 on the far-right-hand side.) XPS (Figure S2c) indicates that there were on average 1.6 F atoms per W atom on the AD surface and that F completely desorbed in the redox process. This residual fluorine from the WF_6 precursor can explain the lateral disorder. If W has varying numbers of F atoms in the AD state instead of being all-O-bonded (as in the Ox and Re states), the W lateral position should shift away from the missing O, preventing lateral correlation. Oxidation removed all F atoms and caused the W^{6+} cations to migrate to the unoccupied B sites. O-bonded W cations are locked in B sites, and the thermodynamics is evidently such that W^{6+} cations do not exchange with Fe cations in A sites. In the Re state, the top O of the O−Fe−O_3−Fe··· substrate surface could be removed by 2% H_2 to form an Fe−O_3-Fe··· surface. However, the transition from Fe−O_3−Fe to O−Fe−O_3−Fe is very easy.[14] Thus, in the Re state, the substrate surface is also O−Fe−O_3−Fe···. XPS indirectly demonstrates this by showing no change in the Fe spectra in going from the Re to the Ox state. Furthermore, W^{5+} is more or less like Fe in surface-terminated Fe═O, and our XSW measurements indicate that a fraction of the W^{5+} replaces Fe in A sites (and that perhaps some Fe can migrate to B sites). This causes the migration of W from B sites to A sites. Thus, W^{5+} cations equally occupy both A and B sites in the Re state. Reoxidation returns W^{6+} to the previous structure in the Ox state.

In summary, using the first XSW case study of ALD-grown WO_x on α-$Fe_2O_3(0001)$, we have demonstrated redox-driven cation dynamics for a catalyst on an oxide support. In situ XSW atomic imaging shows that for $^1/_3$ ML W, (1) 70% of the W atoms are correlated to the hematite lattice, (2) the reduced surface has W cations equally occupying the A and B Fe sites, and (3) oxidation causes all of the W cations in A sites to move to B sites with redox reversibility. Ex situ XPS shows that the W cations are in the 5+ and 6+ oxidation states for the respective reduced and oxidized surfaces. Reversibility was observed in this redox process, which demonstrates its relevance to catalytic applications.

Acknowledgment. This work was supported by the Institute for Catalysis in Energy Processes (U.S. DOE Grant DE-FG02-03ER15457) and MRSEC (NSF Grant DMR-0520513). X-ray measurements were performed at Argonne National Laboratory (U.S. DOE Grant DE-AC02-06CH11357), APS stations 5ID-C, 5BM-D, 12ID-C, and 33ID-D.

Supporting Information Available: Substrate preparation; ALD growth; and AFM, XSW, XRF, XPS, and XAFS characterization. This material is available free of charge via the Internet at http://pubs.acs.org.

References

(1) Weckhuysen, B. M.; Keller, D. E. *Catal. Today* **2003**, *78*, 25.
(2) Bond, G. C.; Tahir, S. F. *Appl. Catal.* **1991**, *71*, 1.
(3) Banas, J.; Tomasic, V.; Weselucha-Birczynska, A.; Najbar, M. *Catal. Today* **2007**, *119*, 199.
(4) Bedzyk, M. J.; Cheng, L. W. *Rev. Mineral. Geochem.* **2002**, *49*, 221.
(5) Cheng, L.; Fenter, P.; Bedzyk, M. J.; Sturchio, N. C. *Phys. Rev. Lett.* **2003**, *90*, 255503.
(6) Fiedor, J. N.; Proctor, A.; Houalla, M.; Hercules, D. M. *Surf. Interface Anal.* **1995**, *23*, 204.
(7) Kim, C.-Y.; Elam, J. W.; Pellin, M. J.; Goswami, D. K.; Christensen, S. T.; Hersam, M. C.; Stair, P. C.; Bedzyk, M. J. *J. Phys. Chem. B* **2006**, *110*, 12616.
(8) Batterman, B. W. *Phys. Rev. Lett.* **1969**, *22*, 703.
(9) Golovchenko, J. A.; Patel, J. R.; Kaplan, D. R.; Cowan, P. L.; Bedzyk, M. J. *Phys. Rev. Lett.* **1982**, *49*, 560.
(10) Zegenhagen, J. *Surf. Sci. Rep.* **1993**, *18*, 202.
(11) Woodruff, D. P. *Rep. Prog. Phys.* **2005**, *68*, 743.
(12) Kim, C.-Y.; Escuadro, A. A.; Stair, P. C.; Bedzyk, M. J. *J. Phys. Chem. C* **2007**, *111*, 1874.
(13) Bergermayer, W.; Schweiger, H.; Wimmer, E. *Phys. Rev. B* **2004**, *69*, 195409.
(14) Rohrbach, A.; Hafner, J.; Kresse, G. *Phys. Rev. B* **2004**, *70*, 125426.
(15) Lemire, C.; Bertarione, S.; Zecchina, A.; Scarano, D.; Chaka, A.; Shaikhutdinov, S.; Freund, H.-J. *Phys. Rev. Lett.* **2005**, *94*, 166101.

JA906816Y